MICRO-VIBRATION PERFORMANCE PREDICTION OF SEPTA24 USING SMESIM (RUAG SPACE MECHANISM SIMULATOR TOOL)

Manolo Omiciuolo, Andreas Lang, Stefan Wismer, Stephan Barth, & Dr. Gerhard Székely

RUAG Schweiz AG, Schaffhauserstrasse 580 CH-5082, Email: gerhard.szekely@ruag.com

ABSTRACT

Scientific space missions are currently challenging the performances of their payloads. The performances can be dramatically restricted by micro-vibration loads generated by any moving parts of the satellites, thus by Solar Array Drive Assemblies too. Micro-vibration prediction of SADAs is therefore very important to support their design and optimization in the early stages of a programme. The Space Mechanism Simulator (SMeSim) tool, developed by RUAG, enhances the capability of analysing the micro-vibration emissivity of a Solar Array Drive Assembly (SADA) under a specified set of boundary conditions. The tool is developed in the Matlab/Simulink® environment throughout a library of blocks simulating the different components a SADA is made of. The modular architecture of the blocks, assembled by the user, and the set up of the boundary conditions allow time-domain and frequency-domain analyses of a rigid multi-body model with concentrated flexibilities and coupled-electronic control of the mechanism. SMeSim is used to model the SEPTA24 Solar Array Drive Mechanism and predict its micro-vibration emissivity. SMeSim and the return of experience earned throughout its development and use can now support activities like verification by analysis of micro-vibration emissivity requirements and/or design optimization to minimize the micro-vibration emissivity of a SADA.

Keywords: micro-vibration emissivity, Solar Array Drive Assembly, rigid multi-body simulation, mechatronics modelling, micro-vibration testing, correlation.

1. INTRODUCTION

Scientific missions rely more and more on payloads with very high expected performances (e.g. spatial resolution, spectral resolution, position and pointing accuracy) [1]. Those performances, thus the mission goals, are affected by several physical phenomena induced by both the space environment and the space segment, namely the spacecraft and all its sub-systems [2]. One key phenomenon driving the performances of a payload is the so called micro-vibration load. The micro-vibration load is generated by any moving part integrated into the satellite, and transferred via the structural path of the bus to the payload interface, thus potentially endangering the functional behaviour of the instrument.

The definition of the micro-vibration environment is largely dependent on the properties of the system, subsystem or equipment under consideration, however it is reasonable to talk about micro-vibration loads (forces and torques) as long as the frequency range of interest is [0:500] Hz, the forces level of interest is below 100-200 N down to 1e-3 N, and the torques level of interest is below 20 Nm down to 1e-4 Nm, [3] [4] [5]. The latest tendency seems to focus more and more on levels of loads even lower (down to 1e-6 Nm and 1e-5 N) and to a frequency range of [0:200] Hz. Such a tendency is driven mainly by the micro-vibration susceptibility of the optical payloads of new generation in the range [5:200] Hz [6], and by the Attitude Orbit Control Subsystem in the range [0:5] Hz. Micro-vibrations term refers therefore to the broadband and the low level disturbance that is able to excite the structural modes of a system subjected to such environment [7], thus increasing the noise experienced by the spacecraft instruments and subsystems.

There are two fields of importance: micro-vibration susceptibility and emissivity. The first is the capability of a system to fulfil its functionalities within the required performances' envelope under the micro-vibration loads transferred to that system via its interfaces. The second is a set of micro-vibration loads a system can generate during its operation, and transfer to the platform via its interfaces.

This paper focuses on the topic of micro-vibration emissivity to Solar Array Drive Assemblies. A Solar Array Drive Assembly (SADA) is an equipment of the Electric Power Subsystem (EPS) of a spacecraft [2]. Its common physical architecture consists of three key components: the Solar Array Drive Mechanism (SADM), and the Solar Array Drive Electronics (SADE) that drive the Solar Array (SA). A SADA can be described as an electromechanical kinematic chain, thus generating disturbance loads with levels of the same order of magnitude of the loads mentioned above, and in the frequency range addressed by the micro-vibration definition.

The susceptibility of the payloads leads to flow micro-vibration emissivity requirements down to all the moving parts of a satellite that contribute eventually to the overall micro-vibration emission budget of a spacecraft. The SADAs are constrained by micro-

vibration emission requirements more and more stringent, to be verified by analysis and/or by test. Tab. 1 provides an example of requirement flowed down to SADA level.

Table 1.Example of micro-vibration emission requirement for a SADA.

Frequency [Hz]	Torque around rotation axis FFT [Nm]	Torque around other axes FFT [Nm]	Forces FFT [N]
0-0.05	<5e-5	<1e-6	<1e-5
0.05-1	<5e-4	<1e-6	<1e-5
1-5	<5e-2	<1e-6	<1e-5
5-35	<5e-3	<1e-6	<1e-5
35-100	<2e-4	<1e-6	<1e-5

The verification of the micro-vibration requirements by test implies the availability of facilities enabling the measurement of very low level loads in a frequency range highly sensitive to any surrounding disturbances (e.g. subways or trains if passing close to the facility, air conditioning systems, electrical net, other tests). Moreover the lowest micro-vibration emissivity levels (as per Tab. 1) could easily fall in the noise range of the facility, thus weakening the reliability of any measurement [3]. Moreover the tribology aspects intrinsically present in a space mechanism [10] (e.g. lubrication), would require to test the system in the worst case environmental conditions of the mission (e.g. temperature range, vacuum pressure, free fall gravity field). References [3] and [8] present the European state of the art in terms of best micro-vibration facilities available now. Tab. 2 summarizes the current capabilities versus the needs identified for the near mid-term space mission micro-vibration field of investigation and testing.

Table 2. Current capabilities versus needs.

Feature	Current	Need
Temperature	Ambient	Cold
Pressure	Soft vacuum	Vacuum
Mission gravity field	1g gravity	Free fall
Frequency range	2-3 up to 500 Hz	1e-2 up to 500 Hz
Lowest reliable force resolution	1e-3 N	1e-5 N
Lowest reliable torque resolution	1e-4 Nm	1e-6 Nm
Measurement accuracy	5% in the allowed ranges	5% in the full ranges

Central point of this paper is to present the process adopted to improve the capability of verifying micro-vibration emissivity requirements of a SADA by analysis. The process is implemented exploiting the current capabilities of the available test facility at ESTEC [3], adopting RUAGs simulator tool called SMeSim (Space Mechanism Simulator) capable of simulating a SADA under its operational conditions, and correlating the simulation results against real measurements carried out on a SEPTA24 SADM [9] controlled in full step and in micro-step mode.

2. THE SMESIM TOOL

2.1. Introduction

A SADA is usually built out of the following components:

- SADE;
- SADM:
    - Chassis/Structure;
    - Motor (a permanent magnet stepper motor for the SEPTA24);
    - Gear Box (a Harmonic Drive 1:160 for the SEPTA24);
    - Slip Ring Assemblies (for the Power and the Signals);
    - Position Sensors (a potentiometer and a reset switch for the SEPTA24);
- Mechanical interface the SA (Solar Array) is fixed to.

Thanks to its modularity the SMeSim tool can simulate any parameterized electromechanical mechanism like a SADA relying on the same philosophy a rigid multi-body with concentrated flexibilities model is built with. The flexibilities represent:

- Joints (e.g. coupling flexibilities);
- Torsion body flexibility by means of splitting the body into two rigid body linked through a spring and a damper (torsional eigen-mode).

The SMeSim tool can be used to perform the following analyses:

- Time-domain analyses;
- Frequency-domain analyses;
- Micro-vibration analyses: a post-processing routine allows the user to represent the micro-vibration emissivity loads (forces, torques, FFTs) at the SADM interface to the spacecraft, as well as the parameterization allows the execution of sensitivity analyses and/or DoE to identify the major contributing parameters which is part of this paper;
- Motorization analyses.

2.2. Functional Architecture of the SMeSim Tool

The SMeSim tool is conceived first at functional level as a Dynamics Performance Model (DPM). The IDEF0 (Integrated DEFinition for Functional Modelling [11]) model of the tool is driven by the key function of the

tool, that is to provide its services. The decomposition of this key function leads to the representation of Fig. 1, where the function "simulate SADA/SA" can be further decomposed down to "simulate SADE", "simulate SADM", and "simulate SA". The decomposition of "simulate SADM" leads to the representation of Fig. 2.

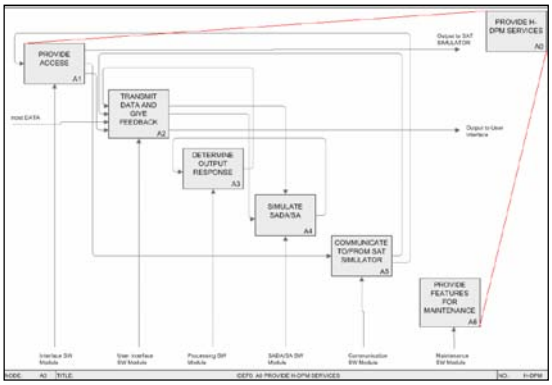

Figure 1. IDEF0 Chart of SMeSim Tool.

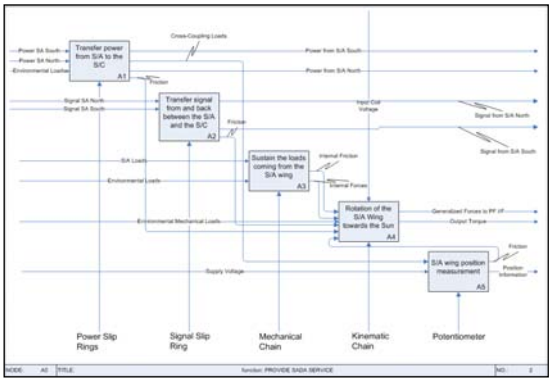

Figure 2. IDEF0 Chart of a SADM.

The IDEF0 approach helps in the preliminary identification of shortfalls (absence of needed functionalities) and overlaps (redundancy in functionalities). The functional charts is used to trace the use case scenarios (operational view) of the tool onto the functional view, thus verifying the solution (the tool) addresses properly the needs identified in the early phase of its realization.

2.3. Model Based Software Engineering of SMeSim

The design and implementation of the SMeSim tool is realized in the Matlab/Simulink® block diagram environment. The design technique is driven by the need to make the simulator easily used for further Hardware-in-the-Loop (HITL) simulations. Therefore a fixed time step size solver is selected to avoid problems of missing error conditions if C-codes is generated or a real-time simulation (e.g. Hardware-in-the-loop, rigs) is executed. On the other hand the fixed step size solver can generate integration problems each time the dynamic behaviour of a model changes rapidly (e.g. friction models, non linearity models). The selection of a suitable time step size is therefore a key aspect of the simulation to:

- Avoid numerical integration problems due to non linearity models;
- Catch all the meaningful physical phenomena frequencies modelled without aliasing.
- Avoid any memory allocation error due to the storage capability of Matlab/Simulink® **.mat* files.

A SADA has to perform continuous rotations at different speeds (for a GEO Orbit the nominal speed is of 1 rev/day at the output of the SADA). The micro-vibration frequency range of interest is [0:500] Hz, therefore a time step frequency of at least 10 kHz is recommended and applied.
A library of blocks simulating the SADA components is built. The multi-domain simulation of a SADA is based on the recombination of the blocks keeping the following approach:

- States are always transferred in forward from a block to the next one;
- Generalized forces are always transferred in feedback from a block to the previous one.

In such a way a block *j* is linked to the block *j-1* and *j+1* only as shown in Fig. 3. The approach just mentioned eases the implementation of a component-by-component modelling. That helps the correlation to breadboard mechanisms (e.g. a breadboard with a motor and the gear box only can be easily reproduced by the tool simply hiding the effect of the blocks simulating the other components of the chain, slip rings and solar wing) test results.

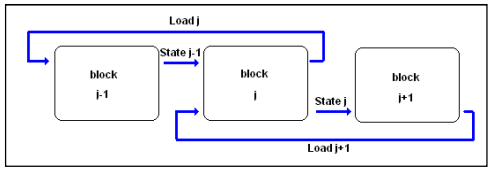

Figure 3. Topology Approach for the SMeSim tool.

The following components are modelled and represented by a Simulink® block:

- Permanent Magnet Stepper motor;
- Driver Electronics (SADE);
- Gear Box (Harmonic Drive) and Ball Bearings;
- Slip Rings (Power and Signal);
- Flexible Body Appendage (Solar Array).

2.3.1. Stepper Motor

The Permanent Magnet Stepper Motor is modelled by Eq. 1 [12]:

$$J_r \cdot \ddot{\varphi} + b_m \cdot \dot{\varphi} + T_{mh} \cdot \frac{\dot{\varphi}}{|\dot{\varphi}|} = T(\varphi, i_j) + T_d - T_L \quad (1)$$

The state of the rotor is represented by the angular position, the angular velocity, and the angular acceleration $\{\varphi, \dot{\varphi}, \ddot{\varphi}\}$. The following contributors and dependencies are modelled:

- Rotor inertia J_r;
- Motor mechanical and electrical damping constant b_m;
- Magnetic hysteresis factor T_{mh};
- Detent torque T_d;
- Torque saturation against current *T_L*;
- Temperature dependencies of the electrical parameters [13].

The electrical circuit of one of the coil (*j*) of the Stepper Motor is modelled by Eq. (2), taking into account the resistance of the coil (*R*), the inductance (*L*), and the counter-electromotive force (V_{emf}) [12].

$$V_j(t) = R \cdot i_j(t) + L \cdot \frac{di_j(t)}{dt} + V_{emf,j}(t) \qquad (2)$$

The block simulating the Permanent Magnet Stepper Motor receives the commanded voltage from the foregoing block (SADE), and the load from the next block (Gear Box). It provides with a set of parameters among which the state $\{\varphi, \dot{\varphi}, \ddot{\varphi}\}$ is transmitted to the next block.

2.3.2. Drive Electronics

The Drive Electronics is modelled taking into account the different control modes a Stepper Motor can undergo:

- Voltage control full step mode;
- Current control full step mode;
- Current control micro step mode.

The voltage control full step mode is realized through a look-up table in which the parameter *width* is used to select the amount of duty cycle used, and *pstep* is used to associate the step size. The voltage signal, V_{peak}, is an input to the Stepper Motor block.

The current full step control mode is realized by means of a similar look-up table using I_{peak} instead of V_{peak}. The generated reference current law is processed by the SADE block currently modelled as a Proportional Integrative (PI) control loop. The SADE generates the right voltage signal to command the Motor minimizing the error between the current reference signal (I_{peak}) and the coil current signal (I_1 and I_2 of Eq. (2)).

The current micro step control mode is realized using Eq. 3 to generate the reference signal as a function of the simulation time (t_{sim}), and the motor frequency (f_m).

$$I_1 = I_{peak} \cdot \cos\left(\frac{2 \cdot \pi}{4} \cdot f_m \cdot t_{sim}\right) \qquad (3)$$

$$I_2 = I_{peak} \cdot \sin\left(\frac{2 \cdot \pi}{4} \cdot f_m \cdot t_{sim}\right)$$

The reference current signal is then transformed from continuous to discrete form by means of the desired number of microsteps.

2.3.3. Gear Box

The Gear Box (a Harmonic Drive for SEPTA24) and the bearings are modelled taking into account the following phenomena [14]:

- Compliance of the gear box;
- Friction of bearing sets;
- Friction of the gear-tooth meshing;
- Structural damping of the gear box;
- Backlash or play among teeth (almost negligible for a Harmonic Drive).

The Harmonic Drive of the SEPTA24 SADM is ideally conceived as a box with two inputs and two outputs (as shown in Fig. 4), respectively:

- Wave Generator angle displacement and rate, $\varphi_{wg}, \dot{\varphi}_{wg}$ (input);
- Flex Spline torque, or better said, the external load coming from the next body, T_{fs} (input);
- Flex Spline angle displacement and rate, $\varphi_{fs}, \dot{\varphi}_{fs}$ (output);
- Wave Generator torque, or better said the load acting on the motor rotor, T_{wg} (output);

The motor rotation is clearly an input because it is transmitted through the Wave Generator by a reduction mechanism to the flexible spline. However the amount of torque transmitted through the system is governed by the amount of torque applied to the flex spline [14]. The statement can be understood assuming no output torque, no friction and losses. The input torque is necessarily zero. This statement has a general validity over all the gear box systems [14].

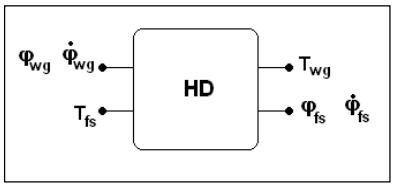

Figure 4. Ideal Harmonic Drive of the SEPTA24.

The complete model takes into account the following phenomena:

- Friction due to input SADM ball bearings, as a contribution of static and viscous friction;
- Friction due to wave generator ball bearing (input ball bearing), as a contribution of static

and viscous friction (T_{f1} in Fig. 5);

- Friction due to gear-tooth meshing, as a contribution of Stribeck, static and viscous friction (T_{f2} in Fig. 5);
- Structural damping of the flex spline (T_{st} in Fig. 5);
- Friction due to output SADM ball bearings, as a contribution of static and viscous friction (T_{f3} in Fig. 5);
- Torsional stiffness of the Harmonic Drive (K_{fs} in Fig. 5);
- All the intermediate transmitted torques at the key nodes of the HD chain (wave generator, flex spline).

The topological layout [14] of the Harmonic Drive is shown in Fig. 5.

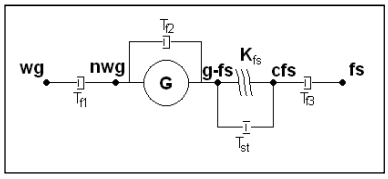

Figure 5. Harmonic Drive Model [14].

Concerning the friction models applied to simulate the wet lubricated Harmonic Drive and the wet lubricated Ball Bearing [9] of the SEPTA24, the following models are selected:

- Static-Viscous (typically used for ball bearings);
- Stribeck-Static-Viscous (typically used for gear-tooth meshing).

Friction parameters are set to the values identified within the qualification campaign of the SEPTA24 [9].

2.3.4. Solar Array

The Solar Array is a flexible body characterized by several eigen-frequencies and eigen-modes. A Finite Element model of the SA shall give the eigen-frequencies, the principal directions of the eigen-modes, and the amount of mass and/or inertia participating to the eigen-modes. The SMeSim is conceived to take the first torsional mode into account, thus simulating:

- the global behaviour of the Solar Array in terms of a generic output torsional load;
- the local torsional vibration behaviour of the Solar Array;

Fig. 6 shows the scenario that drove the model and physical assumptions SMeSim is based on.

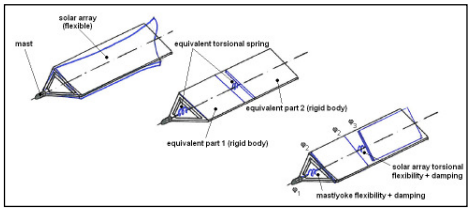

Figure 6. SA Modelling Assumption.

Eccentricities of mechanical components and eccentricities due to manufacturing uncertainty are taken into account as additional factors playing a crucial role in the micro-vibrations emissivity of the SADA. Such eccentricities can generate reactions forces and cross-torques at the interface of the SADA to the spacecraft that could disturb the entire frequency range of interest as well as introduce additional disturbance torques at the centre of gravity (CoG) of the satellite. The model shown in Fig. 7 is one example of eccentricity of a SA. The eccentricity of the SA is driven by the SA and the yoke mechanical configuration.

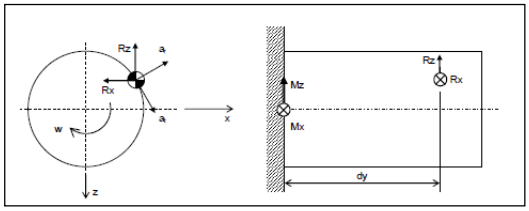

Figure 7. Example of Solar Array eccentricity model.

2.3.5. Model Topology

Fig. 8 shows the SMeSim topology of SADA equipment provisioned with the SEPTA24 SADM.

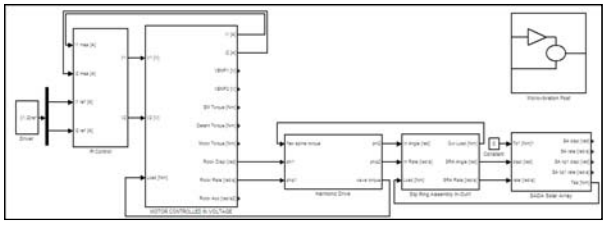

Figure 8. SMeSim representation of SADA.

Each parameter of the SMeSim is followed by an uncertainty parameter in order to keep the status of an analysis consistent with the level of knowledge of a physical parameter. ECSS uncertainty parameters are considered too in case a motorization analysis has to be carried out.

The modelling, simulation, storage, and post-processing of the reactions forces and torques along the three axes at the interface of the SADA (F_x, F_z, T_x, T_y, T_z) is the final and key information provided by the SMeSim tool to allow the micro-vibration analysis.

3. SMESIM VERIFICATION AND VALIDATION

3.1. V&V Approach

Verification and validation of the tool that will be used itself to support the verification process of the system it simulates, is conducted through the following steps:

- Verification: assessment of the SMeSim that its behaviour and characteristics complies with its specified requirements, especially the ability to reproduce the system;
- Validation: determining that the design process produced the right simulation system, based on the needs expressed by the stakeholders [11], (the users and the department).

Verification is carried out through simulations of the different blocks (different components of the SADA) and assessment of the level of accuracy of the simulation results against available test results and/or literature data.
Validation is carried out through a practical use of the SMeSim tool in the frame of a SEPTA24 running programme, aiming at assessing micro-vibration of the SADM alone and a complete SADA equipment under specified operational conditions.

3.2. SMeSim Verification

The SMeSim verification relies on the ability of reproducing the components of a SADA. Fig. 9 shows the comparison of the SMeSim outcome for a stepper motor controlled in full step current mode, and in micro-step current mode, both with a given I_{peak} value and a given frequency.

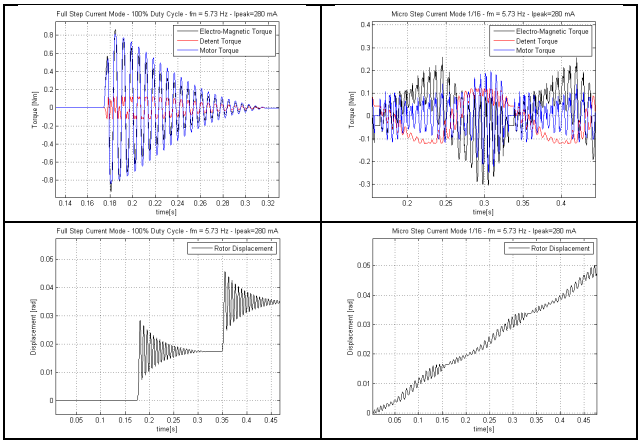

Figure 9. SMeSim Verification – Stepper Motor.

Fig. 9 shows that the micro-step control mode leads to torques exerted by the motor of magnitude lower than the full step mode. Moreover the motion of the rotor is as expected smoother for the micro-step mode.
The modularity of the SMeSim and the capability to simulate different electro-mechanical devices is verified in the frequency domain too simulating an actuator different from the SEPTA24. Fig. 10 shows the comparison of the FFT of the exported torques of the SEPTA33 actuator simulated versus tested at a given condition (stepper motor frequency of 100 Hz). The frequency accuracy appears to be lower than 2 Hz, whereas the amplitude accuracy appears to be worth improving, at least for certain frequencies. The verification in the time domain is though pretty good as shown in Fig. 11.

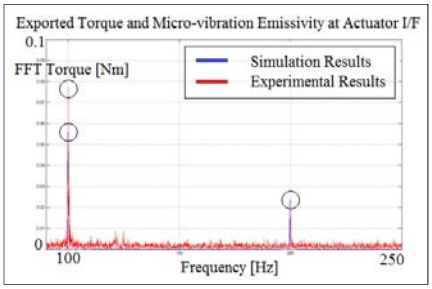

Figure 10. SMeSim Verification – Exported Torques.

motor frequency f=100 Hz	SMeSim	Experimental SN001/SN002 Average	Error
Worst Case Voltage	10.4 V	10.1 V	2.9%
Worst Case Current	23.41 mA	24.98 mA	6.3%
Worst Case Torque	0.140 Nm	0.138 Nm	1.5%
Current @ 26VDC	127.1 mA	120.18 mA	5.7%
Torque @ 26VDC	0.692 Nm	0.634 Nm	9%
Motor Margin	4.94	4.66	6%

Figure 11. SMeSim Verification – Time Domain.

All the blocks belonging to the SMeSim library undergo the verification approach illustrated above, providing good confidence on the simulation tool and justifying the further validation process. This is done through a correlation of each individual component (e.g. gear box, bearings) with test data to reduce uncertainty for certain key figures such as friction, damping, stiffness.

3.3. SMeSim Validation

The key need of the SMeSim is to allow any user verifying a micro-vibration emissivity requirement by analysis. Fig. 12 shows the conceptual roadmap of the validation.

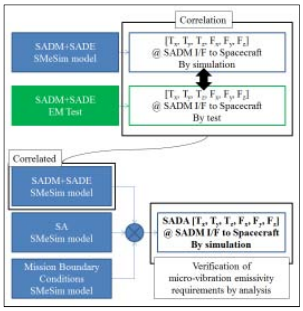

Figure 12. SMeSim Validation – Concept.

The validation relies on the simulation-test correlation driven by the current capability of the test facility: conducting a micro-vibration emissivity test in thermal vacuum cold/hot conditions is today not possible, as well as carrying out the test holding a full scale SA dummy. The correlation is therefore carried out under the operational conditions allowed by state of the art of the test facilities. The SMeSim model parameters are then tuned to be representative of the actual mission boundary conditions (e.g. temperatures, friction values, electro-magnetic constants), and the model itself is enhanced with a block simulating the meaningful dynamics of the SA. The SMeSim model is then used to simulate the complete SADA-SA equipment and get its micro-vibration emissivity prediction in both the time and frequency domain (via FFT algorithms).
Fig. 13 shows tested and simulated micro-vibration torque emissivity about the rotation axis according to the certain parameters associated to the test campaign.

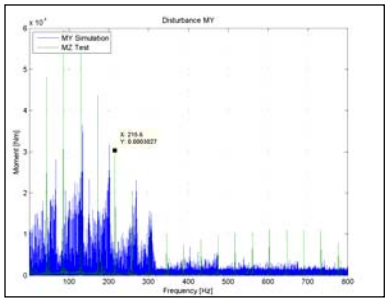

Figure 13. Output speed 1 rev/day, 64 µsteps 190 mA (The rotation axis is Y for SMeSim, Z for the test).

Fig. 13 shows the model suffers a spread of frequency resolution compared to the clear peak of the test. This is due to the time resolution modelling of the drive electronics that can be improved by the use of a block full representative of the driving electronics.

4. SEPTA24 PERFORMANCE ASSESSMENT

SMeSim is used to carry out Design of Experiments (DoE) simulations aiming at generating a characterization of the micro-vibration emissivity budget of a SADA with the SA and the SADE parameterized as indicated in Tab. 3.

Table 3. DoE - Parameterization of SA and SADE.

Solar Array	***SADE***
Inertia along the rotation axis	Steps Mode [1, ½, ¼, 1/8, 1/16, 1/32, 1/64]
1st eigenfrequency along the rotation axis	Peak Current Level

Fig. 14 shows the result of a DoE with modified number of micro-steps, and keeping all the other parameters the same for all the simulations. The higher the number of micro-steps the lower the amplitude of micro-vibration emissivity across a wide frequency range, low and high.

Fig. 15 to 18 show the result of a DoE modifying the inertia and the 1st frequency of the Solar Array about the rotation axis, for a motor frequency of 0.7 Hz (64 micro-steps, 0.4 A peak current).

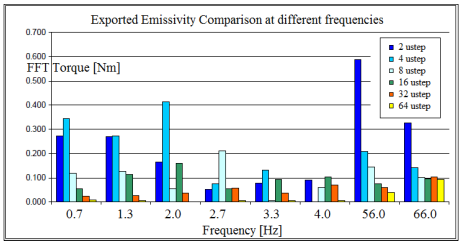

Figure 14. DoE SADE.

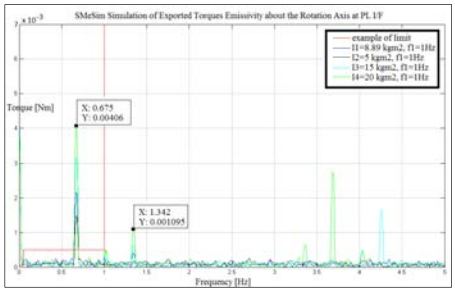

Figure 15. DoE SA [0:5]Hz.

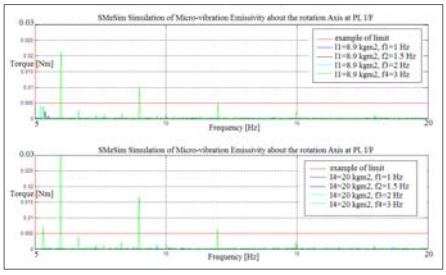

Figure 16. DoE SA [5:20]Hz.

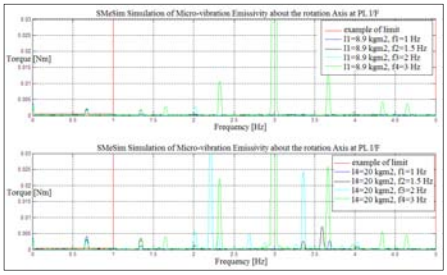

Figure 17. DoE SA [0:5]Hz.

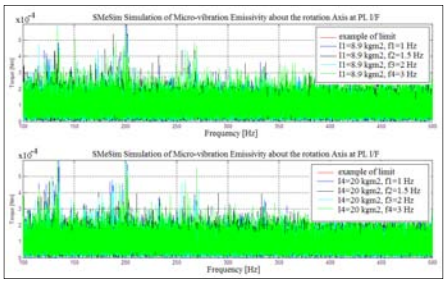

Figure 18. DoE SA [100:500]Hz.

The DoE shows that the SA inertia impacts the low frequency range [0:20] Hz, amplifying the amplitude at the main motor frequency and its harmonics. The 1st torsional frequency of the SA can be used to shift peaks in this range whenever their amplitude is beyond a required level. The SA plays a negligible role in the higher frequency range [20:500] Hz.

5. LESSON LEARNED AND CONCLUSIONS

The activity described in this paper shows that the main contributors of the SADA low frequency range emissivity (<20 Hz) about its rotation axis are the main motor frequency, the gear box stiffness, and the SA. The harmonics of the motor and the friction noise of the bearings and gear box matter in the high frequency range (>20 Hz). The verification and validation of SMeSim show that simulation accuracy is largely dependent on how good the model is representative of the different components. The windowing functions used to generate the FFTs have also an impact on the frequency and amplitude accuracy, therefore they must be selected considering the signal and the driving parameter (a flat top is used as it is the best for a sinusoidal signal, minimizing spectral leakage and improving the amplitude accuracy) [15].
Besides the promising results, SMeSim can be further improved when the emissivity along the other two axes (perpendicular to the rotation axis) needs to be assessed. The refinement of the already implemented simplified equations of the cross-couplings dynamics among the three axes is the next logic step to provide the SMeSim with such an improvement. Indeed each phase of a programme should be associated to a certain level of acceptable accuracy in order to maximize the return of information against the simulation and correlation effort. A paradigm is proposed in Tab. 4:

Table 4. Simulation Accuracy.

Programme Phase	***Frequency Accuracy***	***Amplitude Accuracy***
Preliminary Study	±5 Hz	≤ 30%
PDR	± 2 Hz	≤ 20%
CDR	± 0,5 Hz	≤ 10%
Test Phase - DRB	± 0,1 Hz	≤ 5%

The paper shows an approach that is currently supporting the verification by analysis of micro-vibration emissivity requirements in a running programme. Nonetheless the verification by test of current and future micro-vibration emissivity requirements will be enabled by the enhancement of the existing micro-vibration test facilities according to the needs showed in Tab. 2.

6. ACKNOWLEDGEMENT

The author thanks the co-authors and the SEPTA24 team for the support and the shared effort.

7. REFERENCES

1. Post-MSG Project Team EUMETSAT (2007), *MTG Mission Requirements Document v2C*, http://www.eumetsat.int/groups/pps/documents/document/pdf_mtg_mrd.pdf.
2. J.R.Wertz and W.J. Larson,Space *Mission Analysis and Design*, 3rd edition, Space Technology Library.
3. M. Wegner, S. Airey, G. Piret, P. Le (2012), *ESA New Reaction Wheel Characterization Test Facility (RFC)*, 35th Annual AAS Guidance and Control Conference.
4. A. Defendini, L. Vaillon, F. Trouve, Th. Rouze, B. Sanctorum, G. Griseri (1999), *Technology Predevelopment for active control of vibration & very high accuracy pointing systems*, 4th ESA Spacecraft GNCS Systems Conference.
5. M. Vitelli, B. Specht, F. Boquet (2012), *A process to verify the microvibration and pointing stability requirements for the Bepi Colombo mission*, ESA International Workshop on Instrumentation for Planetary Mission.
6. M. Toyoshima, Y. Takayama, H. Kunimori, T. Jono, S. Yamakawa (2010), *In-orbit measurements of spacecraft microvibrations for satellite laser communication links*, Optical Engineering Journal, Vol. 49, Issue 8.
7. Paolo Gaudenzi (2009), *Smart Structures: Physical behavior, Mathematical Modeling and Applications*, J. Wiley and Sons, p. 164.
8. M. Privat (1999), *On ground and in orbit microvibrations measurement comparison*, Proc. 8th ESMATS, Vol. 438, p.181.
9. E. Gasperini, B. Heinrich, W. Weisenstein, A. Oriol (2011), *Qualification of the SEPTA24 high power SADA*, ESMATS 2011, Proceedings.
10. P. L. Conley (1998), *Space Vehicle Mechanisms Elements of Successful Design*, J. Wiley and Sons.
11. Buede D.M. (2009), *The Engineering Design of Systems, John Wiley*, New York.
12. P. Acarnley (2007), *Stepping Motors, a guide to theory and practice*, 4th ed., IET Control Engineering Series 63
13. R.H.Welch Jr, G.W.Younkin (2002), *How temperature affects a Servomotor's Electrical and Mechanical Time Constants*, Industrial Controls Consulting Division, Bullseye Marketing Inc, Industry Application Conference.
14. H.D. Taghirad, P.R. Bélanger (1998), *A Nonlinear Model for Harmonic Drive Friction and Compliance*, 1998 IEEE International Conference on Robotics and Automation.
15. S. Stergiopoulos (2009),*Advanced Signal Processing Handbook: Theory and Implementation for Radar, Sonar, and Medical Imaging Real Time Systems,* Electrical Engineering & Applied Signal Processing Series.